

2014

# Adaptive-feedback spectral-phase control for interactions with transform-limited ultrashort high-power laser pulses

Cheng Liu

*University of Nebraska-Lincoln, cliu8@unl.edu*

Jun Zhang

*University of Nebraska-Lincoln*

Shouyuan Chen

*University of Nebraska-Lincoln, schen6@unl.edu*

Grigory V. Golovin

*University of Nebraska-Lincoln, ggolovin2@unl.edu*

Sudeep Banerjee

*University of Nebraska-Lincoln, sbanejee2@unl.edu*

*See next page for additional authors*

Follow this and additional works at: <http://digitalcommons.unl.edu/physicsumstadter>

 Part of the [Physics Commons](#)

---

Liu, Cheng; Zhang, Jun; Chen, Shouyuan; Golovin, Grigory V.; Banerjee, Sudeep; Zhao, Baozhen; Powers, Nathan D.; Ghebregziabher, Isaac; and Umstadter, Donald, "Adaptive-feedback spectral-phase control for interactions with transform-limited ultrashort high-power laser pulses" (2014). *Donald Umstadter Publications*. 99.  
<http://digitalcommons.unl.edu/physicsumstadter/99>

This Article is brought to you for free and open access by the Research Papers in Physics and Astronomy at DigitalCommons@University of Nebraska - Lincoln. It has been accepted for inclusion in Donald Umstadter Publications by an authorized administrator of DigitalCommons@University of Nebraska - Lincoln.

---

**Authors**

Cheng Liu, Jun Zhang, Shouyuan Chen, Grigory V. Golovin, Sudeep Banerjee, Baozhen Zhao, Nathan D. Powers, Isaac Ghebregziabher, and Donald Umstadter

# Adaptive-feedback spectral-phase control for interactions with transform-limited ultrashort high-power laser pulses

Cheng Liu, Jun Zhang, Shouyuan Chen, Gregory Golovin, Sudeep Banerjee, Baozhen Zhao, Nathan Powers, Isaac Ghebregziabher, and Donald Umstadter\*

Department of Physics and Astronomy, University of Nebraska-Lincoln, Lincoln, Nebraska 68588, USA

\*Corresponding author: donald.umstadter@unl.edu

Received October 28, 2013; accepted November 12, 2013;  
posted November 25, 2013 (Doc. ID 198894); published December 20, 2013

Fourier-transform-limited light pulses were obtained at the laser-plasma interaction point of a 100-TW peak-power laser in vacuum. The spectral-phase distortion induced by the dispersion mismatching between the stretcher, compressor, and dispersive materials was fully compensated for by means of an adaptive closed-loop. The coherent temporal contrast on the sub-picosecond time scale was two orders of magnitude higher than that without adaptive control. This novel phase control capability enabled the experimental study of the dependence of laser wakefield acceleration on the spectral phase of intense laser light. © 2013 Optical Society of America

OCIS codes: (140.3590) Lasers, titanium; (140.7090) Ultrafast lasers; (320.5520) Pulse compression; (320.7100) Ultrafast measurements.

<http://dx.doi.org/10.1364/OL.39.000080>

Advanced laser technologies such as Kerr-lens mode-locking [1] and chirped pulse amplification (CPA) [2] have led to the generation and amplification of extreme light pulses that are capable of supporting large spectral bandwidths. The availability of ultrashort pulses (femtosecond) of high-power (petawatt) laser light has enabled novel experimental research in high-field physics, including relativistic nonlinear optics, laser-driven accelerators, and secondary radiation sources [3].

The spectral phase, which determines the temporal pulse shape, is a critical laser parameter that needs to be controlled and optimized for the high intensity laser matter interaction. For instance, in order to optimize the performance of laser-wakefield accelerators (LWFA), the laser pulse duration is required to match the plasma period of the accelerator medium [4]. The efficiency of an LWFA also depends on the detailed shape of the driving laser pulse [5]. As the spectral phase also controls the pulse temporal contrast ratio, it affects the results in high-field physics experiments due to the preionization [6]. Interactions that depend on the carrier frequency, which are affected by laser pulse chirp, also require spectral phase control.

In terms of the CPA laser pulse compression, it is difficult to remove all of the high-order phase distortions by only tuning the stretcher/compressor parameters. Several technologies have recently been demonstrated to precisely control the spectral phase for ultrafast laser pulses [7–10]. In particular, an adaptive spectral phase closed-loop feedback system has the capability to measure the spectral phase using a self-referenced spectral interferometer (SRSI) [11], and it is able to precisely control the spectral phase by means of an acoustic optic programmable dispersive filter (AOPDF) [7].

Experiments that use high-power laser pulses must be performed in vacuum in order to prevent degradation of the laser pulse on account of nonlinear effects during propagation in air. However, the current spectral phase control methods which are used under atmospheric and low-power conditions are not compatible with high-field experiments. Therefore, a complete and systematic

method is imperative to fully characterize and control the spectral phase and temporal shape of the on-target high-power pulses for high-field physics experiments under vacuum conditions.

We demonstrate an adaptive closed-loop system that controls the spectral phase of laser pulses from a 100 TW laser system. Pulses with both ideal temporal shape and enhanced coherent contrast were obtained at the location of the target in vacuum. We have used the spectral phase control system to experimentally investigate the dependence of the LWFA electron beam characteristics on the chirp of the laser pulse, which has been recently studied using modeling and simulations [12].

The schematic of the experimental setup for the spectral-temporal measurement is depicted in Fig. 1. The 100-TW laser system consists of a broadband oscillator, an Öffner-type stretcher, and four stages of amplifiers able to deliver 5 J per pulse before compression at a

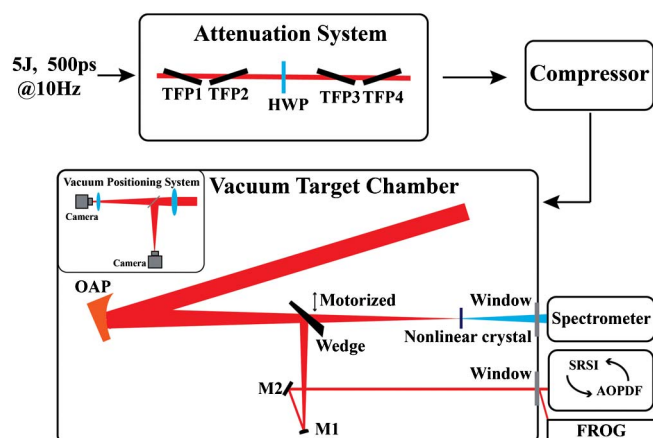


Fig. 1. Schematic of the experimental setup for temporal profile measurement with spectral phase closed-loop. TFP1-4, thin-film polarizers; HWP, half-wave plate; OAP, off-axis parabolic mirror; M1, gold-coated convex mirror,  $f = -100$  mm; M2, 45° gold-coated plane mirror; SRSI, self-referenced spectral interferometer. The spectral phase was measured by Wizzler and feedback to Dazzler as closed-loop. The SHG and XPW spectra were measured after each cycle of the feedback loop.

repetition rate of 10 Hz. An acoustic optic programmable dispersive filter (AOPDF) (*Dazzler*, Fastlite Inc.) was installed before the stretcher to precompensate for the gain-narrowing effect in the laser amplifiers and to maintain the desired spectral phase for the amplified laser pulse at the output of the system. A Treacy-type grating pair compressor recompressed the stretched pulses to a femtosecond scale. An  $f/14$  off-axis parabolic mirror was used to focus the beam on the target. A beam positioning system was installed in the vacuum chamber to monitor and control the near-field position and far-field pointing of the laser beam.

A half-wave plate (HWP) and thin-film polarizers (TFPs) attenuation system was implemented before the compressor to sample the high-power beam, thus, ensuring that the lower and higher power beams had the same optical properties. A set of two TFPs were installed before the HWP in the attenuation system to eliminate the modulated spectral portion with crossed polarization [13]. The HWP and second pair of TFPs were used to adjust the energy scale in the experiments. The loss in beam energy for the four TFPs was measured to be less than 5%, which can be neglected for a laser system with an output of 5 J per pulse. A broad and deep hole in the spectrum appeared when the HWP was set to minimize the transmission energy (zero position) because of the limited extinction ratio of the HWP and TFPs within the entire spectral range [14]. The HWP was then set to  $5^\circ$  from the zero position to keep the same spectral shape as that at full-power.

The high-power laser beam was then transported into the experimental vacuum chamber. A part of the beam from the off-axis parabolic reflector that focuses the beam on target was reflected by a wedge. This was guided to the measurement device by means of a convex mirror and a plane mirror assembly that down collimates the beam to the desired diameter. The beam exits a window in the vacuum chamber to the measurement device. The dispersion of the window was accounted for in measurements of the temporal pulse duration.

For these measurements the B-integral was not a concern since all reflective optics were used. The pulse energy was attenuated to less than  $100 \mu\text{J}$  by the attenuation system without altering the temporal and spectral properties of the high-power laser pulse. The spectral phase was measured using SRSI (*Wizzler*, Fastlite Inc.) for each laser shot. The spectral phase information was extracted from the spectral interference between the initial pulse and its crossed-polarized wave (XPW) pulse [11]. An adaptive spectral phase closed-loop between the SRSI and AOPDF, using the measurement from the SRSI to set the phase imparted by the AOPDF on the pulse, was implemented in order to compensate for the residual dispersion from the entire laser system.

With the feedback loop in operation, the SRSI was used to measure the temporal pulse duration. The result of this measurement is shown in Fig. 2(a), and the pulse duration was 32 fs. This is in agreement with the Fourier-transform-limited (FTL) pulse duration that is expected based on the spectral shape and bandwidth of the incident laser pulse. An independent measurement of the pulse duration was performed using the technique of frequency-resolved optical gating (FROG) (*GRENOUILLE*, Swamp Optics), and

the results are shown in the left inset of Fig. 2(a). This measurement results in a measured value of 32 fs for the pulse duration, which is in agreement with the SRSI measurement. Figure 2(b) shows the temporal profile of the pulse as measured by the Wizzler. In addition to obtaining an FTL pulse, the coherent contrast on the  $\pm 400$  fs time-scale was improved by two orders of magnitude, when the spectral phase was corrected using the feedback system (CL), as compared to the optimal pulse duration without spectral phase correction (OL). The pulse duration in the latter case was 33 fs. This result represents a significant step forward compared to prior work that improved the coherent contrast on picosecond time scale by proper choice of stretcher optics [15]. Such active feedback techniques will be critical in experiments where the coherent pedestal has undesirable effects on the target before its interaction with the high-intensity laser pulse.

The spectral phase with adaptive spectral phase control as shown in Fig. 3(a) illustrates the spectrum of the laser pulse, the modulated spectral phase, and the flat phase that was obtained with feedback correction. The flat spectral phase corresponds to the FTL pulse in the temporal domain and this corresponds to compensation of all spectral orders that distort the phase during amplification and propagation in the laser chain. As noted above, both conditions produced nearly identical temporal durations, but the flat spectral phase led to a significant suppression of the coherent pedestal on femtosecond time scales.

Similar to the pulse duration which was independently measured using the FROG technique, we verified the validity of the measurement using independent techniques based on second harmonic generation (SHG) [8,10] and XPW generation [16]. The SHG and XPW spectra at the target point with different frequency chirp values were measured in vacuum. For the SHG measurement, a type I phase-matching beta barium borate (BBO) crystal

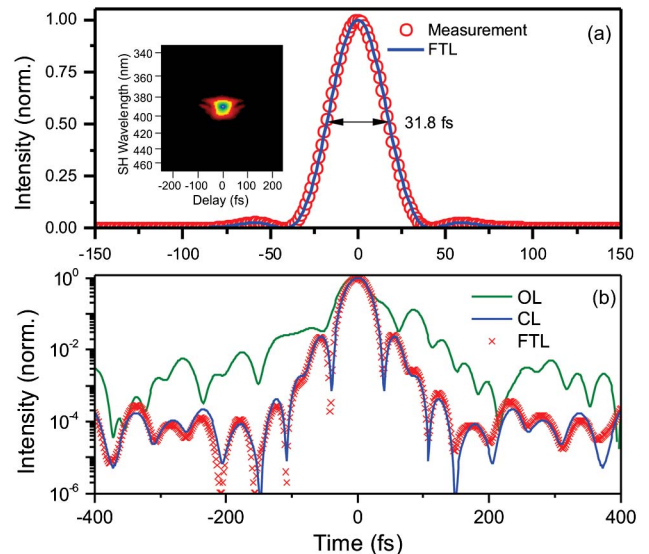


Fig. 2. Measurement results of pulse duration and coherent contrast. (a) Temporal profile with spectral phase closed-loop. The upper-left inset shows the trace from the SHG FROG, which gives almost the same result of 32 fs. (b) Coherent contrast with feedback (CL), without feedback (OL), and the theoretical FTL pulse (FTL).

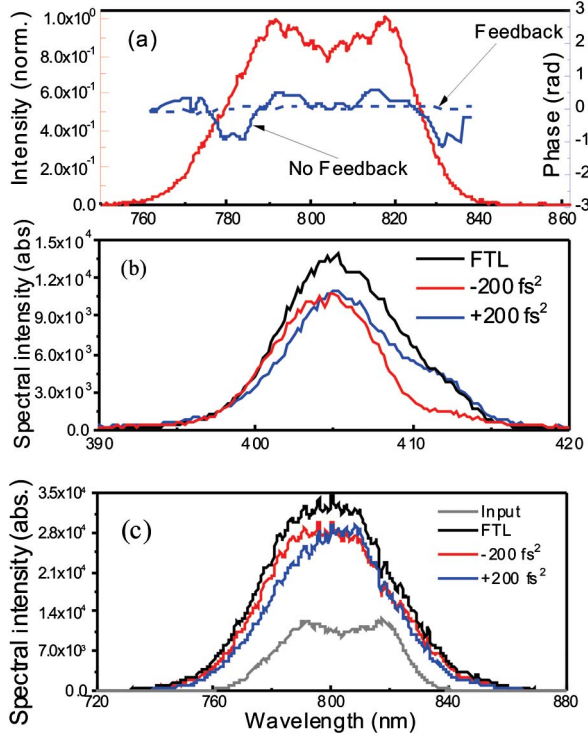


Fig. 3. Spectral properties of the on-target pulses. (a) Measurement spectrum (red line) and spectral phase before (solid blue line) and after (dashed blue line) feedback. (b) SHG and (c) XPW spectra for cross-checking the FTL pulse at the target point.

(50  $\mu\text{m}$  thickness;  $\theta = 29.2^\circ$ ;  $\varphi = 0^\circ$ ) was placed at the target point in the vacuum chamber.

Figure 3(b) shows the SHG spectra for three different chirp values at  $-200 \text{ fs}^2$ ,  $0$ , and  $+200 \text{ fs}^2$ . Zero chirp corresponds to the FTL pulse. The bandwidths of the SHG spectra were nearly identical for all three cases and maximum conversion efficiency was measured for FTL pulses. An XPW crystal ( $\text{BaF}_2$ , 1 mm long, (011)-cut) was also placed at the target point. Figure 3(c) shows the XPW spectra respectively at  $-200 \text{ fs}^2$ ,  $0$ , and  $+200 \text{ fs}^2$ . The spectra for the three frequency chirp values were all broadened by the XPW effect. We observed both the broadest spectrum and highest XPW conversion when there was no frequency chirp in the pulse, which is consistent with the results in [17]. The measurements made with the SRSI, FROG, SHG, and XPW validate our claim that a transform-limited pulse was obtained at the interaction point.

Since we were able to obtain a flat phase laser pulse on the target and control the different order phases separately using the adaptive phase control method, this enabled us to study the dependence of laser-wakefield-accelerated electron beams on the laser chirp without ambiguity. A 2.4 J laser pulse was focused on a 0.5 mm mixed gas target (1% nitrogen and 99% helium) with an intensity of  $5 \times 10^{19} \text{ W/cm}^2$ . Electrons were injected into a laser wakefield via an ionization assisted injection mechanism [18]. The chirp of the laser pulse was changed from  $-600 \text{ fs}^2$  to  $+1000 \text{ fs}^2$ . The typical electron beam energy spectrum generated at each chirp is shown in Fig. 4. This result revealed that a positive chirp helps to

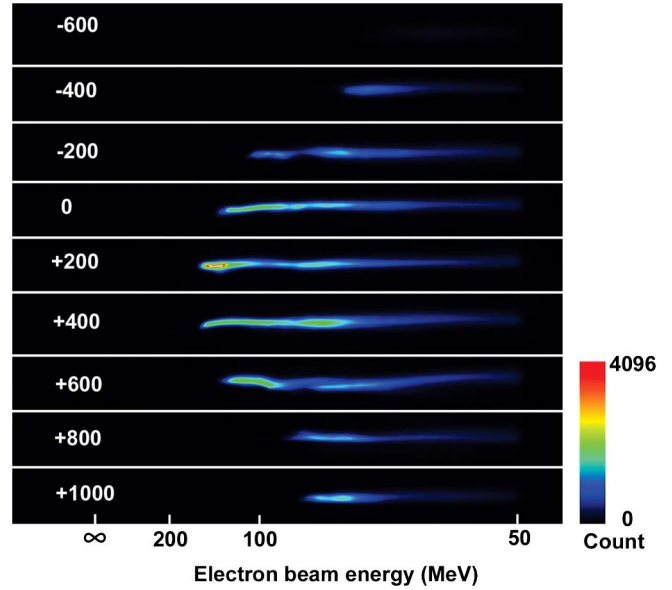


Fig. 4. Dependence of laser chirp on the generation of quasi-monoenergetic electron beams. The pulse chirp was scanned from  $-600 \text{ fs}^2$  to  $+1000 \text{ fs}^2$  while fixing other laser and accelerator parameters. It shows that the electron beam cutoff energy and charge above 50 MeV is asymmetric with respect to the zero chirp.

generate an electron beam with higher cutoff energy and charge. For this experiment,  $+200 \text{ fs}^2$  was the best chirp parameter for electron beam generation. The asymmetrical behavior of the electron energy and charge showed that the frequency chirp played a critical role in LWFA. While the detailed physics of this type of dependence will be discussed in a forthcoming report, this phase dependence experiment demonstrates the importance of this phase control technology in the study of high-intensity laser-plasma interaction.

In conclusion, a spectral phase closed-loop was implemented for a 100-TW CPA laser system, and the temporal properties of the laser pulse under vacuum conditions were fully characterized in this study. An FTL temporal pulse and coherent contrast were obtained. To the best of our knowledge, this is the first time spectral phase control has been used to obtain an FTL temporal laser pulse in vacuum for a 100-TW-level laser system. The ability to precisely control the temporal characteristics of the laser pulse on target in vacuum enabled investigation of the dependence of LWFA performance on the temporal shape and frequency chirp. This work will have applications in future high-field physics experiments that require ultrashort pulses and controllable characteristics.

We thank K. Brown, J. Mills, and C. Petersen for their contributions to the laser facility. This work was supported by U.S. DOE Grant No. DE-FG02-05ER15663, DTRA Contract No. HDTRA1-11-C-0001, and AFOSR Grant No. FA9550-11-1-0157.

## References

1. D. E. Spence, P. N. Kean, and W. Sibbett, *Opt. Lett.* **16**, 42 (1991).
2. D. Strickland and G. Mourou, *Opt. Commun.* **56**, 219 (1985).

3. G. Mourou, T. Tajima, and S. Bulanov, *Rev. Mod. Phys.* **78**, 309 (2006).
4. V. Malka, *Phys. Plasmas* **19**, 055501 (2012).
5. D. Umstadter, E. Esarey, and J. Kim, *Phys. Rev. Lett.* **72**, 1224 (1994).
6. J. Bromage, C. Dorrer, and R. Jungquist, *J. Opt. Soc. Am. B* **29**, 1125 (2012).
7. P. Tournois, *Opt. Commun.* **140**, 245 (1997).
8. V. V. Lozovoy, I. Pastirk, and M. Dantus, *Opt. Lett.* **29**, 775 (2004).
9. D. Nguyen, M. Piracha, and P. Delfyett, *Opt. Lett.* **37**, 4913 (2012).
10. Y. Wu, E. Cunningham, H. Zang, J. Li, M. Chini, X. Wang, Y. Wang, K. Zhao, and Z. Chang, *Appl. Phys. Lett.* **102**, 201104 (2013).
11. T. Oksenhendler, S. Coudreau, N. Forget, V. Crozatier, S. Grabielle, R. Herzog, O. Gobert, and D. Kaplan, *Appl. Phys. B* **99**, 7 (2010).
12. V. B. Pathak, J. Vieira, R. A. Fonseca, and L. O. Silva, *New J. Phys.* **14**(2), 023057 (2012).
13. X. N. Zhu, M. Piche, G. D. Goodnob, and R. J. D. Miller, *Opt. Commun.* **145**, 123 (1998).
14. Y. Zhao, Y. Jia, J. Yang, and X. Zhu, *Opt. Eng.* **46**, 044301 (2007).
15. C. Hooker, Y. Tang, O. Chekhlov, J. Collier, E. Divall, K. Ertel, S. Hawkes, B. Parry, and P. Rajeev, *Opt. Express* **19**, 2193 (2011).
16. A. Jullien, L. Canova, O. Albert, D. Boschetto, L. Antonucci, Y.-H. Cha, J. P. Rousseau, P. Chaudet, G. Cheriaux, J. Etchepare, S. Kourtev, N. Minkovski, and S. M. Saitiel, *Appl. Phys. B* **87**, 595 (2007).
17. L. Canova, O. Albert, N. Forget, B. Mercier, S. Kourtev, N. Minkovski, S. M. Saitiel, and R. Lopez Martens, *Appl. Phys. B* **93**, 443 (2008).
18. A. Pak, K. A. Marsh, S. F. Martins, W. Lu, W. B. Mori, and C. Joshi, *Phys. Rev. Lett.* **104**, 025003 (2010).